Comparison of Total Performances for High-Speed EMS-type Magnetically Levitated Railway Vehicle

* Shinichi KUSAGAWA, * * Jumpei BABA, * Katsuhiko SHUTOH, * Eisuke MASADA

*Department of Electrical Engineering, Faculty of Science & Technology
Tokyo University of Science
2641 Yamazaki, Noda, Chiba 278-8510, Japan
Tel: +81-4-7124-1501 ext. 3767 / Fax: +81-4-7124-1810
E-Mail : kusagawa@emasada.ee.noda.tus.ac.jp, shutoh@ee.noda.tus.ac.jp,
masada@ee.noda.tus.ac.jp
**Department of Electrical Engineering, Faculty of Science & Technology
The University of Tokyo
7-3-1 Hongo, Bunkyo-ku, Tokyo 113-8656, Japan
Tel: +81-3-5841-6563 / Fax: +81-3-5841-8575, E-Mail : baba@asc.t.u-tokyo.ac.jp

Keywords – Control Performance, Electromagnetic suspension, Magnetic levitation and Vehicle weight reduction.

Abstract

Because high-speed operation of maglev vehicle causes large variation of gap length with high frequency, it requires high magnet current and its high-speed control. On the other hand, the reduction of total weight of a vehicle is key issue for realization of high-speed maglev system with the short stator propulsion principle. To solve these problems keeping its control performance to cope with high-speed operation, three types of control schemes are discussed and compared. With simulation results of maglev operational performances, it is shown that proposed schemes enable to reduce the weight of magnets and current controllers as well as keeping its control performances.

1 Introduction

A type of the magnetically levitated railway system (MAGLEV) with the electro-magnetic suspension system (EMS), which is named HSST, will be put into revenue service as an urban transport in Nagoya, Japan at the beginning of April 2005 [1]. Its maximum speed is limited to 100km/h, though its running test operations have been completed up to 130km/h. However, in order to extend its applications into the high speed and middle distance system in the future, the design of its EMS system is reexamined for improvement of riding comfort and performances of a train.

On the other hand, the reduction of the total weight of vehicle is key issue for realization of high-speed maglev system with the short stator propulsion principle. Because the weight of magnets, including supporting structures and current controllers, occupies considerable part of the total weight, its reduction with introduction of a new control scheme is studied.

Fig. 1. New HSST Vehicle for TKL levita-

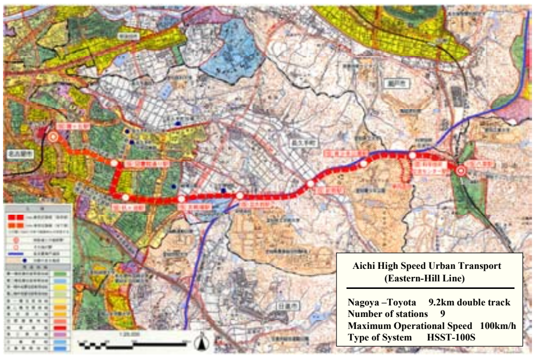

Fig. 2. Route Profile of Eastern Hillside Line (TKL) in Nagoya, Japan (9.2km).

Because high-speed operation of maglev train causes large variation of gap length with high frequency, it requires high magnet current and its high-speed control. However it makes the weight of both magnets and controllers heavier. Then the drive unit of maglev becomes heavier. From this reason, the weight of levitation system inevitably should be reduced. To solve these mutually contradicting objectives, novel control schemes (based on hybrid control scheme and fuzzy control) for the levitation system are proposed over the conventional one, control parameters of which are optimized both to follow the track exactly in high speed and to provide enough riding comfort to passengers.

2 Numerical model

2.1 Magnetic Levitation Model

To clarify the fundamental characteristics of proposed schemes, a simplified model, one body is supported by two modules as shown in Fig. 3, is used on the basis of HSST system [2]. For the running direction of the vehicle, the module that places former part of the body is called as “front module”, and the other is called as “rear module”. Four magnets are arranged in line composition per module, which is assumed to be a rigid body in itself and its length is 2.5m. The right-and-left guidance system is excluded from the target as a passive system like HSST-100.

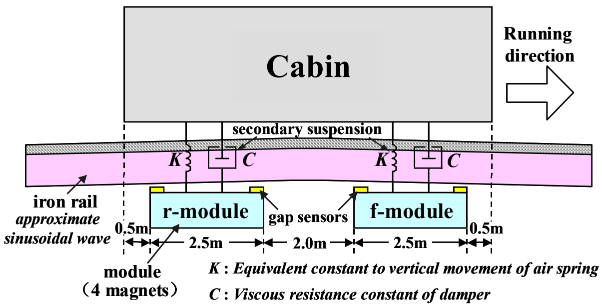

Fig. 3. Magnetic levitation model

It is assumed that secondary suspensions composed of an air-spring K and a damper C are incorporated between the module and the cabin. In addition, gap sensors are assumed to be arranged before and behind the module to improve reliabilities of them. The detected values of gap length are averaged before they are input to the controller in each module.

2.2 Levitation Control System

Fig. 4 shows the control block diagram corresponding to Fig. 3 and Table I shows each parameter for levitation control system. Every parameter in this Table is calculated by referring to the data of HSST-100 [3]. Though the block diagram of rear module isn’t shown, the composition is symmetry in the front and rear module. The variables with subscript "f" correspond to the front module and those with subscript "r" correspond to the rear module.

In Fig. 4, the “*Control Model*” enclosed by dotted line shows the control block diagram of levitating magnets. If the gap length fluctuates Δz from the nominal operating point (z_0, i_0), the deviation of the magnet current Δi and the deviation of the voltage Δe are assumed. On the cabin motion, Δw_g shows the displacement of the cabin position in vertical direction and Δw_φ shows the displacement of pitching mode of the cabin. These two values and the Δz are compared. The output value is applied to the secondary suspension and is fed back to the “*Control Model*” as a variation of an external force.

On the gap length control in Fig. 4, in the electric circuit of the “*Control Model”*, the cascade control is carried out to give the fast-response to the fluctuation of gap length (=Δz), and the current control loop is composed of Current Controller like (1). The gap length is controlled by Lift Controller like (2). In addition, the velocity feedback, which corresponds to the differentiation signal of gap length, is added to the “*Control Model”* to stabilize the responses. Every parameter of both two controllers, including K and C, are optimized by use of GA to satisfy both track following performance and riding comfort of passengers.

$$\text{Current Controller} \quad G_{CC}(s) = C_{CC} \cdot \frac{K_{CC}}{s} \tag{1}$$

$$\text{Lift Controller} \quad G_{LC}(s) = C_{LC} \cdot K_{LC}\left(K + \frac{1}{sT}\right) \tag{2}$$

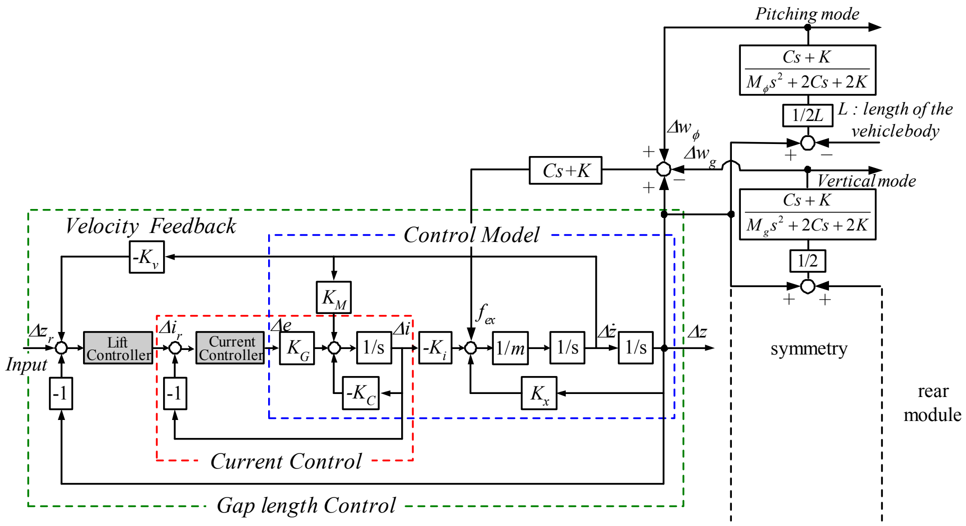

Control of the front module

Fig. 4. Control Block diagram for levitation control system

TABLE I
Parameters for Levitation Control System

Control Model	
Steady-state gap length z_0	8 mm
Excitation current i_0	28.6 A
K_G	8.325 A/V
K_C	5.35
K_i	429.4 N/A
K_x	1535216.4 N/m
K_M	3575 As^2/m
Module (4-magnets)	
Mass (m)	1270 kg
Cabin	
Mass (M_g)	8000 kg
Pitching equivalent mass (M_ϕ)	2000 kg
Secondary Suspension	
K	5000 N/m
C	1220 Ns/m

Controller	
Current Controller	
C_{CC}	100
K_{CC}	1.286
Lift Controller	
K_{LC}	0.00028
T	0.01
C_{LC}	4000
K_p	100
K_V	0.15

2.3 Rail Modeling

Random factors related to the loads of a vehicle are not considered. Only the deflection of the rail is considered as shown in Fig. 5. The span length of the rail is 20 m (= standard value in general), and the deflection at the centre between girders is 2 mm. That is, rail is supposed as a sinusoidal wave with amplitude 1 mm and a period 20 m.

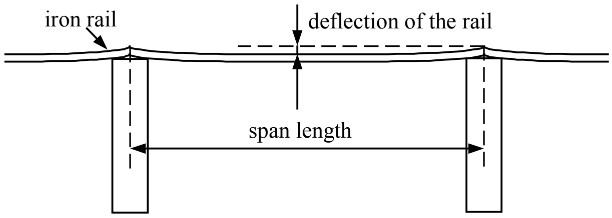

Fig. 5. Deflection of the rail

3 Control Method

3.1 Introduction of Hybrid Control to gap length control

A hybrid control scheme is introduced into the Lift Controller in Fig. 4 to suppress the magnet current against a large gap error signal (as shown in Fig. 6).

The PI controller based on (2) is used for usual rail displacements (for instance, stepped or sinusoidal rail alterations). Control scheme is switched to P control, when an unusual rail alteration occurs and the gap error signal (=Δz_r-Δz) becomes larger than the threshold value (=2mm). This value is determined considering the nominal operating gap length of HSST to be about several mm (6 to10mm). For example, the nominal operating gap length of HSST-100 is 8mm, "2mm" occupies 25% of it and this value cannot be neglected.

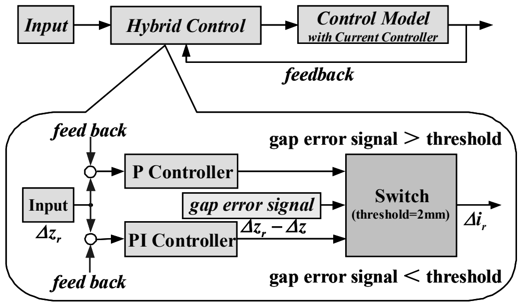

Fig. 6. Concept of hybrid control scheme

3.2 Application of Fuzzy Logic to gap length control

The ability to follow a sharp irregularity of the rail and to cope with high frequency noise in the gap control system should be coordinated with riding comforts. The fuzzy control is introduced into the Lift Controller in Fig. 4 to process the gap error signal to the levitation control system, which can sufficiently follow the large load displacement of the rail. (as shown in Fig. 7.)

It takes three steps to design a fuzzy controller: fuzzyfication, inference rules and defuzzyfication.

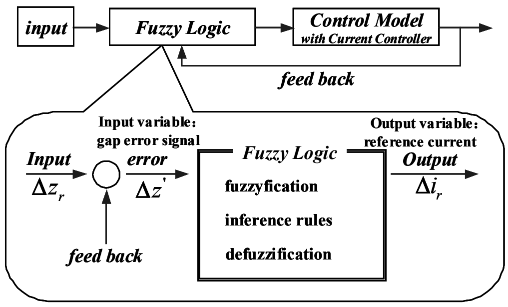

Fig. 7. Concept of gap length control with fuzzy logic

In the first step, the values obtained through the sensors are transformed into the values of corresponding linguistic variables. The second step performs the fuzzy inference giving the linguistic values of the control variables. In the third step, these linguistic values are transformed to the numerical values of the control variable in order to perform the required task. After executing these three steps, the controller is fine tuned in an iterative way. The procedure adopted in this paper is as follows.

The linguistic "input" variable is gap error signal (=$\Delta z'$). The fuzzy set of input has five membership functions (Fig. 8 (a)). With a certain number of membership functions, the control accuracy is just slightly increased, where as too few membership functions make an accurate control impossible. Also with increasing number of membership functions, the rule base becomes bigger therefore increasing the calculation time. The use of Gaussian membership function, in which the grade of the membership function at the centre is assumed to be 1.0 and its own weight changes in inverse proportion to the gap error signal, results in an accurate control with a small number of membership functions. The linguistic "output" variable is the reference current Δi_r, which is applied to the Current Controller after being compared with Δi. Its fuzzy set has also five membership functions as shown in Fig. 8 (b). Mamdani's fuzzy inference method with a max/min rule is used [4].

□*Control Rule*

$$\begin{cases} R_1\text{: If} \quad x \quad \text{is} \quad Gauss_1 \quad \text{then} \quad y \quad \text{is} \quad Gauss_5 \\ R_2\text{: If} \quad x \quad \text{is} \quad Gauss_2 \quad \text{then} \quad y \quad \text{is} \quad Gauss_4 \\ R_3\text{: If} \quad x \quad \text{is} \quad Gauss_3 \quad \text{then} \quad y \quad \text{is} \quad Gauss_3 \\ R_4\text{: If} \quad x \quad \text{is} \quad Gauss_4 \quad \text{then} \quad y \quad \text{is} \quad Gauss_2 \\ R_5\text{: If} \quad x \quad \text{is} \quad Gauss_5 \quad \text{then} \quad y \quad \text{is} \quad Gauss_1 \end{cases}$$

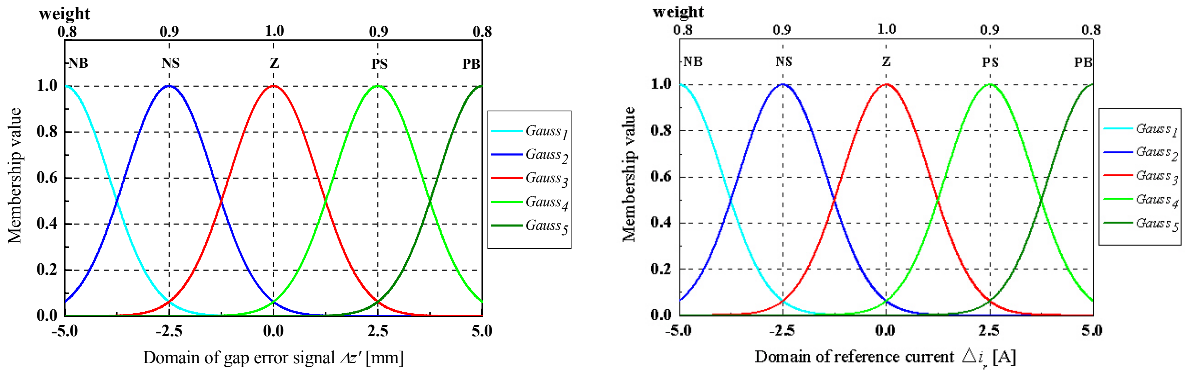

(a) Membership functions of input *x* (b) Membership functions of output *y*

Fig. 8. Membership functions of fuzzy label ([B: big, S: small, N: negative, Z: zero, P: positive])

4 Results of simulation and discussions

To verify the control characteristics of levitation system composed of the preceding chapter, the gap control characteristics are analyzed by running simulations under the following two conditions as particular rail displacements. The running speed of the vehicle is examined in medium-speed area about 200 km/h, which is a future goal in HSST. In this paper, because the kinetic characteristic of rear module is as same as that of front module, only the result of the front module (variable shown by subscript f) is shown.

□Rail detection signal contains noises
□Occurrence of an abnormal value at rail joint

4.1 Noisy case

In [5], the influence on the controllability has been verified when the shape of the rail (amplitude and span length) changes. Here, based on the examination items of [6] and [7], the influence on the control performance is examined when a random vibration (noise) which originates from the surface roughness of the rail is added to the usual rail displacement approximated as a sinusoidal wave according to the velocity of the vehicle and the span length. The displacement of the rail is assumed that the span length is 20m (=standard), with amplitude 2mm and a period 20m.

4.1.1 Running characteristics

Fig. 9 shows the result of comparing the gap length variation (=Δz_f) when the gap detection signal contains noises and is added to the input (=Δz_r) for each control scheme.

In all cases, though some distortions are confirmed in the variation of gap length, it is understood the effect of the noisy input can be removed and stable operation is obtained. However, the following characteristics to the rail with fuzzy control are more excellent than that of other two cases (PI control and hybrid control).

Fig. 10 shows the variation of the magnet current (=Δi) in this case. In the case with fuzzy control, it can be confirmed that an irregular vibration which originates in the noise is induced and its fluctuation range is also large (though the absolute value of the fluctuation amplitude is small) in comparison with other two cases. On the other hand, in two cases with PI control and hybrid control, the peak value of magnet current is significantly removed and its fluctuation amplitude is very small. The optimization of current regulator is also given on the basis of these schemes (PI control and hybrid control).

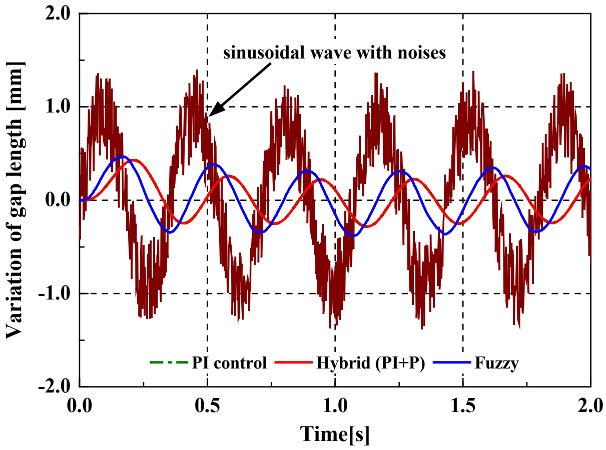

Fig. 9. Variation of gap length against the rail alteration with noises

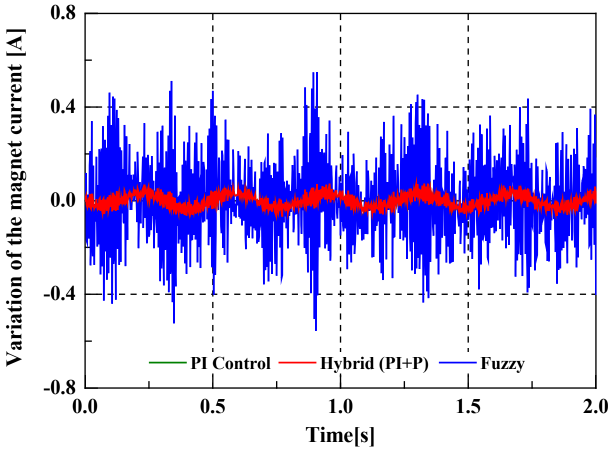

Fig. 10. Variation of the magnet current

4.1.2 The characteristics of riding comfort

To examine the characteristics of riding comfort when the gap detection signal containes noises, the vertical acceleration of the cabin (= $\Delta \ddot{w}_g$) is extracted for each control scheme. The Fourier transformation is applied to the acceleration and the frequency characteristic of its amplitude is obtained by dividing it by the gravity acceleration. As a criterion of riding comfort, the vibration acceleration of JR is used. This criterion and their vertical vibration characteristics of the cabin are compared. The criterion curve of riding comfort is divided into 5 areas according to the coefficient of riding comfort between 1 and 3 (less than 1: very good ～ more than 3: very bad).

Fig. 11 shows the analytical results of riding comfort based on the amplitude of vertical acceleration of the cabin (= $\Delta \ddot{w}_g$) when the gap detection signal containes noises.

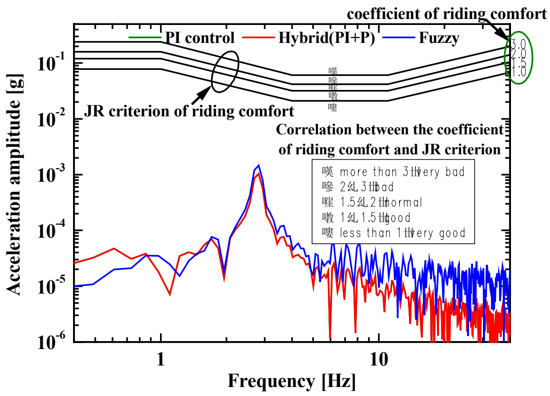

Fig. 11. Frequency characteristics of vertical acceleration of the cabin

It is shown that all of simulated cases satisfied enough riding comfort below the criterion level for JR criterion of riding comfort（acceleration amplitudes in each case are included in area ⑤.）because it is the low or medium speed area below 250 km/h or less in HSST. In the case with PI control and hybrid control, the frequency components that originates in the noisy input are decreased over the wide frequency range and the characteristics of riding comfort are slightly improved compared with the case by use of fuzzy control. Based on Fig. 9 and Fig. 11, a trade-off relation between the running characteristics and riding comfort of passengers can be confirmed.

4.2 Occurrence of an abnormal value at rail joint

There are rail joints between girders and gap exists in them. In addition, it is assumed that this gap length has large amplitude and is considered to be an abnormal value compared with the usual rail displacement approximated as a sinusoidal wave. In addition, it has an ultra minute width for the length between girders. The control performance is examined when this rail alteration is added to the input (=Δz_r).

The size of an abnormal value is assumed to be 5mm from the bottom of the iron rail to the skid considering the nominal operating gap length in HSST, and the width is assumed to be 0.5% (=100mm) of the span length (=20m) between girders.

Fig. 12 shows the conceptual scheme of this rail alteration and Fig. 13 shows the actual input of this rail alteration, which includes an abnormal value. The velocity of the vehicle is 200km/h as an example. The reason why two pulses are detected every one cycle depends on the arrangement and leveling effect of gap sensors. Moreover, though the maximum amplitude of the abnormal value is 5mm, actual input becomes smaller than 5mm because the values detected by before and behind sensors in each module are averaged and then is inputted to Δz_r as a rail displacement signal.

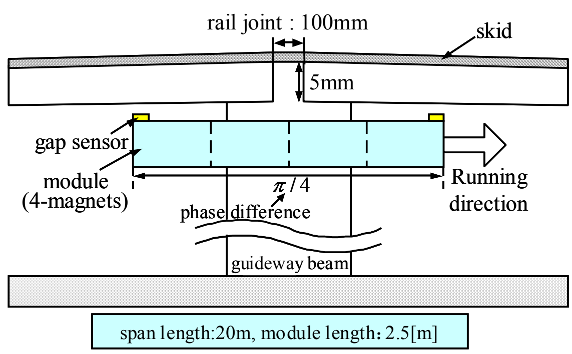

Fig.12. Conceptual diagram of an abnormal rail alteration

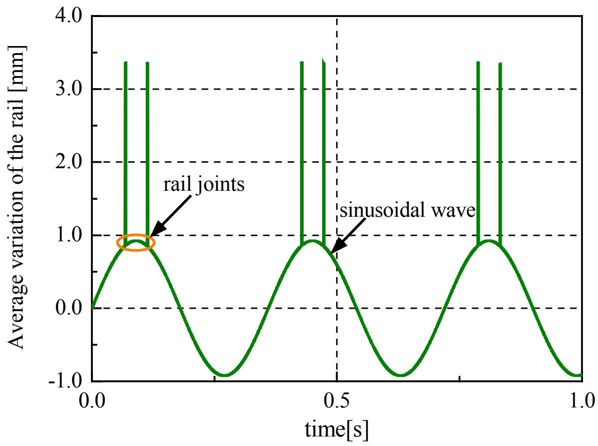

Fig.13. Rail alteration including an abnormal

4.2.1 Running characteristics

On the basis of above assumption, Fig. 14 shows the result of the variation of gap length (=Δz_f) for each control scheme against an abnormal input at rail joint (=Δz_r).

In the case with PI control, the response is suffered drastically by sharp irregular gap signal, causing a large air gap deviation or an offset error to occur. It may affect riding comfort. On the other hand, in two cases with hybrid control and fuzzy control, the effect of the abnormal input can be significantly reduced and variations of gap length are small to be within 1mm in comparison with the nominal operating gap length of HSST-100.

Fig. 15 shows the variation of magnet current (=Δi) in this case. In the case with PI control, steep pulses that originate in the abnormal input appears and a large load may hang to the current controllers etc. On the other hand, in two cases with hybrid control and fuzzy control, the peak values of magnet current are significantly removed and their fluctuation ranges are very small in comparison with the case by use of PI control. The optimization of current regulator is also given on the basis of these schemes (hybrid control and fuzzy control).

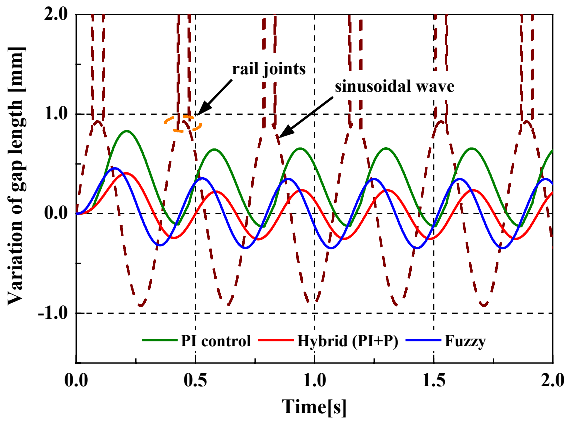

Fig. 14. Variation of gap length against an abnormal input at rail joint

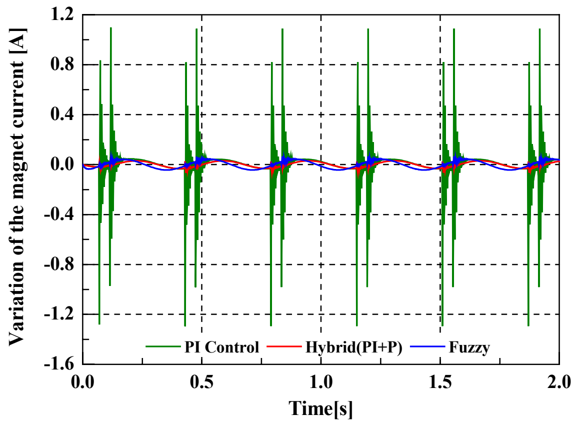

Fig. 15. Variation of the magnet cur-

4.2.2 Riding comfort

Fig. 16 shows the analytical results of riding comfort based on the amplitude of vertical acceleration of the cabin (= $\Delta \ddot{w}_g$) when the abnormal rail alteration occurs.

It is shown that all of simulated cases satisfied enough riding comfort below the criterion level for JR-riding comfort criterion. By the way, in the case with PI control, there are some peaks in high frequency range due to the abnormal input. On the other hand, in two cases with hybrid control and fuzzy control, there are no peaks and the acceleration amplitude is decreased and smoothed over the wide frequency range (including the most human-sensitive band from 4 to 8 Hz).

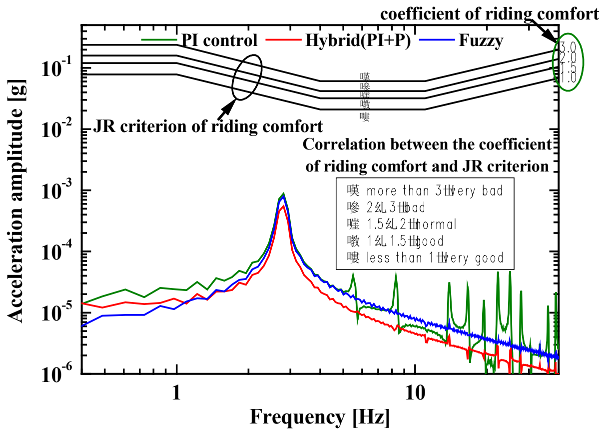

Fig. 16. Frequency characteristics of vertical acceleration of the cabin

4.3 Comparison of Control Performances

On the basis of simulation results, to compare the control performances for three kinds of control methods, the maximum control value and phase delay for each speed are shown in Fig. 17-(a) (noisy case) and Fig. 17-(b) (abnormal case).

In the noisy case, in all cases, the fluctuations of gap length are less sensitive for each speed against the noises included in the gap detection signal.

In the abnormal case, the response is influenced by the abnormal value and its effect is more remarkable as the vehicle speed becomes small in the case with PI control. On the other hand, in two cases with hybrid control and fuzzy control, the fluctuations of gap length are less sensitive for each speed and vehicle operates satisfactorily up to 200km/h.

Next, in both of noisy and abnormal cases, the phase delay becomes large with the rise of speed in two cases with PI control and hybrid control and it becomes a-half cycle in high-speed. This result is not desirable as following characteristics. On the other hand, in the case with fuzzy control, the phase delay becomes very small in comparison with other two methods. It can be said that control performances with fuzzy control are superior to that without fuzzy control.

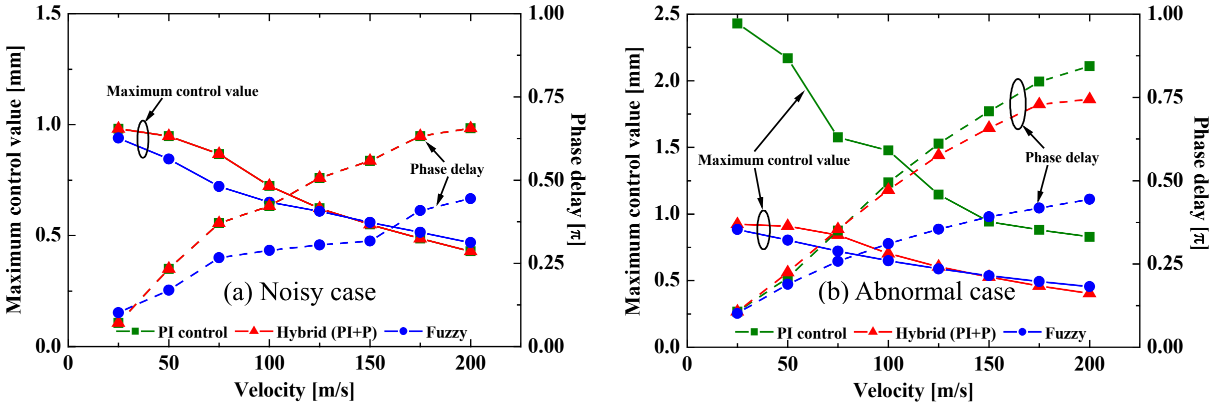

Fig. 17. Comparison of control performances based on maximum control value and phase delay for each

5 The Weight Reduction of Both Magnets and Current Controllers

To evaluate the effect of novel control schemes for weight reduction of both magnets and current controllers of maglev vehicle, the root-mean square value (r.m.s.) and the peak value of magnet current are calculated for three types of control schemes based on Fig. 10 and Fig. 15. Table II summaries the results.

In the noisy case, because the variation of gap length does not exceed the threshold value (=2mm), the control scheme is not switched in hybrid control. As a result, the same results are obtained in PI control and hybrid control. On the other hand, in the case with fuzzy control, the magnet current increases 0.64 % in its r.m.s. value and 2.08 % in its peak value in comparison with the case by use of PI control (basic case).

Next, in the abnormal case, with the introduction of the proposed schemes, the magnet current can be reduced 0.6 % (in hybrid control) and 0.56 % (in fuzzy control) in its r.m.s. value and 4.11 % (in hybrid control and fuzzy control) in its peak value. The r.m.s. current determines the coil winding and the magnet core size consequently. The peak current influences the magnetic saturation of the core, as well as the capacity of the magnet controller. The image of the reduction of magnet volume is shown in Fig. 18.

TABLE II
DIFFERENCES OF MAGNET CURRENT AGAINST THREE TYPES OF CONTROL SCHEMES

Noisy case			
	PI Control	Hybrid Control	Fuzzy Control
r.m.s. [A]	28.6	28.6	28.8
peak value [A]	28.7	28.7	29.3
Abnormal case			
	PI Control	Hybrid Control	Fuzzy Control
r.m.s. [A]	28.79	28.62	28.63
peak value [A]	29.90	28.67	28.67

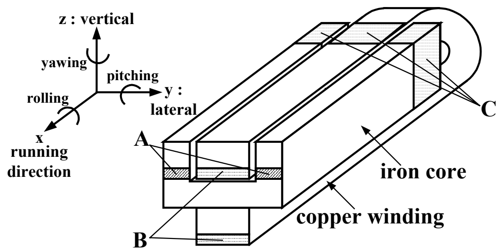

Fig. 18. Image of smaller magnet

Because the cross section of the rail cannot be changed, the reduction of r.m.s. current makes the height of magnet coil lower (the area shown in B) and consequently the height of the core teeth is shortened with the same length (the area shown in A). The reduction of peak current causes the short core length (the area shown in C). The weight reduction of magnet is consequently evaluated about 0.0 % (in hybrid control) and -6.64 % (in fuzzy control) in noisy case and 6.33 % (in hybrid control) and 6.10 % (in fuzzy control) in abnormal case.

The instantaneous power dissipation, which effects on the dimension of magnet controller, can be lowered with the reduction of peak current. Our earlier study based on the data from power electronic devices shows that weight reduction of the magnet controller is nearly proportional to the decrease of its peak power dissipation. Then the weight of the magnet controller is considered to decrease 0.0 % (in hybrid control) and -4.16 % (in fuzzy control) in noisy case and 8.22 % (in hybrid control) and 8.23 % (in fuzzy control) in abnormal case. Table III summarized the results. These devices are designed on the basis of requirements considering maximum allowable number of passengers, allowable number of failed magnets to keep operation and so on. The dynamic behavior of the vehicle in operation is calculated with simulations and modifies the specification on its basis. The worst case is supposed to be included in the basic case.

The practical data of the weight allocation to each component of HSST-100 maglev vehicle shows that the magnets and controllers occupy about 25% of total weight and their ratio is about 2:1. The total weight reduction in magnets and magnet controllers with the hybrid control scheme and fuzzy control are respectively evaluated about 0.0 % and -2.18 % in noisy case and 2.61 % and 2.56 % in abnormal case of the total vehicle weight (HSST-100: 15 ton). Table IV summarizes the results.

These values are not so large. However it is clarified that an appropriate maglev control system design can also contribute the weight reduction of its components and has another meaning to realize a higher speed system. The detailed analysis of the weight of maglev vehicle provides that the improvement of control performance and weight of levitation system can decrease the weight of other components, such as dampers in suspension system. Though the total weight of vehicle is only reduced in about several % (except for the case by use of fuzzy control in noisy case), the synergy effect is expected for the weight of other components; such as the propulsion system also decreases its capacity and weight because of the light vehicle.

TABLE III
WEIGHT REDUCTION OF MAGNETS AND MAGNET CONTROLLERS (BASE: PI CASE)

Noisy case			
	PI Control	Hybrid Control	Fuzzy Control
Magnet [%]		0.00	-6.64
Controller [%]		0.00	-4.16
Abnormal case			
	PI Control	Hybrid Control	Fuzzy Control
Magnet [%]		6.33	6.10
Controller [%]		8.22	8.23

TABLE IV
TOTAL WEIGHT REDUCTION AGAINST THE TOTAL WEIGHT OF VEHICLE (BASE :PI CASE)

Noisy case			
	PI Control	Hybrid Control	Fuzzy Control
Total [%]		0.00	-2.18
Abnormal case			
	PI Control	Hybrid Control	Fuzzy Control
Total [%]		2.61	2.56

6 Conclusion

In this paper, in order to realize a high-speed maglev system with the short stator propulsion principle, which is strong against a large variation of gap length with high frequency, we have proposed to apply three kinds of control methods to an actual HSST-type maglev vehicle and compared with their control performances. As a result, it can be said that proposed methods gives an excellent levitation characteristic in various respects in comparison with the conventional control scheme. The control performance with hybrid control is superior to that of PI control and fuzzy control in terms of realizing good riding comfort, reduction of total weight of a vehicle and energy consumption etc. On the other hand, the control performance with fuzzy control is superior to that of PI control and hybrid control in terms of following characteristics to the rail and stabilities in high-speed operation.

To realize a high-speed maglev system with the short stator propulsion principle, the weight reduction of the vehicle is essential, as well as the improvement of control performance of the levitation system. Application of a novel hybrid control scheme and fuzzy control for maglev is shown to contribute both objectives though a suitable technique for the application field has to be selected considering the trade-off relation between these mutually contradicting objectives. Further studies will be carried out to evaluate the levitation control performance on the total weight reduction of the maglev vehicle in details.

References

1. M. Fujino, M. Tanaka and S. Ishimoto, "Total running test operation of HSST-100 and the project of east hill-side line in Nagoya," Proc. Maglev 2000 in Rio de Janeiro, 2000.
2. E. Masada, J. Fujie, J. Katoh and T. Mizuma, *The technology of the magnetic levitation systems*, Ohm-sha, 1992.
3. S.Kusagawa, J.Baba, K.Shutoh, E.Masada, "Electro-Magnetic Suspension System with Fuzzy Control for a Magnetically Levitated Railway System," Proc.LDIA2003 in Birmingham, UK, (2003).
4. T.Terano, K.Asai, M.Sugeno:"Applied Fuzzy Systems,"Ohm-sha,(1989).
5. S. Kusagawa, J. Baba, K. Shutoh and E. Masada, "Design of EMS-magnetically levitated system based on genetic algorithm," Proc. Maglev 2002 in Lausanne, Switzerland, 2002.
6. "Study Report on Development of Low-pollution Railways Conceptional Design," pp30-73, Ministry of Transportation Japan, (1985).
7. "Study Report on Practical Application of Urban transportation type Linear Motorcar," pp62-132, Practical Application Investigation Committee, (1992).
8. P. K. Shinha, *Electromagnetic suspension dynamics & control*, IEE Control Engineering Series 30, 1987.
9. E. Gottzein, "Das magnetische rad als autonome funktionseinheit modularer Trag- und fuehrsysteme fuer magnetbahnen," Fortschrittberichte der VDI Zeitschriften, Reihe 8, Nr. 68, 1984.
10. S.Kusagawa, J.Baba, K.Shutoh, E.Masada, "Application of Fuzzy Logic to EMS-type Magnetically Levitated Railway Vehicle," IEEJ Trans. on Industry Applications,Vol.124-D,No.4 pp396-404, (2003).